Polarization-modulated analog photonic link with compensation of the dispersion-induced power fading

Haiting Zhang,[1,2] Shilong Pan,[1,*] Menghao Huang,[1] and Xiangfei Chen[1,2]

[1]*College of Electronic and Information Engineering, Nanjing University of Aeronautics and Astronautics, Nanjing 210016, China*

[2]*Nanjing National Laboratory of Microstructures and School of Engineering and Applied Sciences, Nanjing University, Nanjing 210093, China*

**Corresponding author: pans@ieee.org*

Received January 4, 2012; accepted January 11, 2012;
posted January 17, 2012 (Doc. ID 160873); published February 24, 2012

A novel integrable modulator consisting of a polarization modulator and a polarizer is proposed for constructing a high-performance analog photonic link. By adjusting a polarization controller placed before the modulator, both amplitude modulation and phase modulation with adjustable ratio between them are implemented. This feature is used to shift the peak of the frequency response of a dispersive link to any desired frequency, so the dispersion-induced power fading around the frequency is compensated. A proof-of-concept experiment is performed. The compensation of the dispersion-induced power fading in the proposed analog photonic link increases the spur-free dynamic range as large as 12.5 dB. © 2012 Optical Society of America

OCIS codes: 060.2360, 130.4110.

Analog photonic links (APLs) have attracted significant interest in various applications, such as radar systems, wireless communications, and phased array antennas, thanks to the advantages in terms of low insertion loss, broadband, light weight, and immunity to electromagnetic interference as compared with its electronic counterpart [1]. However, chromatic dispersion (CD) of the optical fiber would lead to spectrally periodical power fading because a conventional intensity or phase-modulated APL employs double sideband (DSB) modulation. To reduce the power fading, one method is to use optical single sideband (SSB) modulation [2–7], but a wideband and wavelength-tunable optical SSB modulator is not easily achievable [8]. In [9], the modulation chirp in a directly modulated laser diode (LD) is used to reduce the CD effect in the APLs. However, the frequency chirp in the LD is fixed, so the operation is effective only to APLs with a certain length of fiber or signals at a certain frequency. Recently, a carrier phase-shifted DSB modulation to compensate the dispersion-induced power fading by a dual-parallel Mach–Zehnder modulator (DPMZM) was proposed [10]. The approach can be operated for signals at any frequency, but one of the sub-MZM in the DPMZM must be biased at the minimum transmission point (MITP). The key limitation associated with the operation of an MZM at the MITP is the bias drifting problem, which reduces the system stability.

In this Letter, a novel APL based on an integrable modulator consisting of a polarization modulator (PolM) and a polarizer is proposed and demonstrated. The modulator can perform simultaneously amplitude modulation and phase modulation. The ratio between the two modulations can be adjusted by changing the polarization state of the optical signal introduced to the modulator, which is then used to compensate the dispersion-induced power fading in the APL. An experiment is carried out. The maximum point of the frequency response can be shifted to any frequency of interest. The proposed APL has a spur-free dynamic range (SFDR) improvement as large as 12.5 dB as compared with a conventional intensity-modulation-based (IM-based) link with 20 km single-mode fiber (SMF).

Figure 1 shows the schematic diagram of the novel integrable modulator consisting of a PolM and a polarizer. The PolM is a special phase modulator that can support both TE and TM modes with opposite phase modulation indices [11,12]. When a linearly polarized incident light is oriented at an angle of α to one principal axis of a PolM, complementary phase modulation signals are generated along the two principal axes. The normalized optical field at the output of the PolM along the two polarization axes can be expressed as

$$\begin{bmatrix} E_x \\ E_y \end{bmatrix} = \begin{bmatrix} \cos\alpha \exp[j\omega_c t + j\gamma \cos\omega_m t + j\varphi_0] \\ \sin\alpha \exp[j\omega_c t - j\gamma \cos\omega_m t] \end{bmatrix}, \quad (1)$$

where ω_c is the angular frequency of the optical carrier, γ is the phase modulation index, ω_m is the angular frequency of the modulating signal, and φ_0 is the phase difference between E_x and E_y, which can be changed by adjusting the DC bias of the PolM or a polarization controller (PC) placed before the PolM.

When the complementary signals are sent to a polarizer with its principal axis oriented at an angle of 45° to one principal axis of the PolM, we obtain

$$\begin{aligned} E(t) &= \frac{\sqrt{2}}{2}(E_x + E_y) \\ &= \frac{\sqrt{2}}{2} e^{j\omega_c t}(\cos\alpha e^{j\gamma\cos\omega_m t + j\varphi_0} + \sin\alpha e^{-j\gamma\cos\omega_m t}) \\ &= \frac{\sqrt{2}}{2} e^{j\omega_c t}[\cos\alpha e^{j\varphi_0/2}\cos(\gamma\cos\omega_m t + \varphi_0/2) \\ &\quad + (\sin\alpha - \cos\alpha)e^{-j\gamma\cos\omega_m t}]. \end{aligned} \quad (2)$$

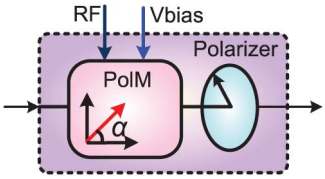

Fig. 1. (Color online) Integrable modulator consisting of a PolM and a polarizer.

As can be seen from Eq. (2), the integrable modulator simultaneously performs amplitude modulation and phase modulation. The ratio between the two modulations can be adjusted by changing α, i.e., the angle of the polarization direction of the incident light and the principal axis of the PolM, which can be implemented by tuning a PC placed before the PolM.

When the signal in Eq. (2) is introduced to a dispersive link, we get

$$\begin{aligned} E(t) = \frac{\sqrt{2}}{2} e^{j\omega_c t}[&J_0(\gamma)(e^{j(\varphi_0+\theta_0)} \cos\alpha + e^{j\theta_0} \sin\alpha) \\ &+ J_1(\gamma) \cos\alpha (e^{j(\omega_m t+\frac{\pi}{2}+\varphi_0+\theta_{+1})} - e^{j(-\omega_m t-\frac{\pi}{2}+\varphi_0+\theta_{-1})}) \\ &+ J_1(\gamma) \sin\alpha (e^{j(\omega_m t+\frac{3\pi}{2}+\theta_{+1})} - e^{j(-\omega_m t-\frac{3\pi}{2}+\theta_{-1})})] \end{aligned} \quad (3)$$

where J_n denotes the nth-order Bessel function of the first kind, θ_0, θ_{+1}, and θ_{-1} are the dispersion-induced phase shifts of the optical carrier, the lower first-order sideband and the upper first-order sideband, respectively [13]. In writing Eq. (3), small-signal modulation is assumed, i.e., higher-order sidebands are neglected. Expanding the propagation constant β in the Taylor series, we have [13]

$$\begin{cases} \theta_0 = z\beta(\omega_c) \\ \theta_{-1} = z\beta(\omega_c) - \tau_0\omega_m + \frac{1}{2}D_\omega\omega_m^2 \\ \theta_{+1} = z\beta(\omega_c) + \tau_0\omega_m + \frac{1}{2}D_\omega\omega_m^2 \end{cases}, \quad (4)$$

where z is the transmission distance, τ_0 is equal to $z\beta'(\omega_c)$, D_ω is equal to $z\beta''(\omega_c)$, and β' and β'' are the first- and second-order derivatives of β with respect to the optical angular frequency.

Applying the optical signal to a photodetector (PD) for square-law detection and ignoring the DC component, we obtain

$$\begin{aligned} i_{\mathrm{PD}} &\propto |E(t)|^2 \\ &= 2J_0J_1\left[\sin 2\alpha \cos\left(\frac{1}{2}D_\omega\omega_m^2\right)\sin\varphi_0 \right. \\ &\quad \left. + \cos 2\alpha \sin\left(\frac{1}{2}D_\omega\omega_m^2\right)\right]\cos\left[\omega_m(t-\tau_0)\right]. \end{aligned} \quad (5)$$

Tuning the DC bias of the PolM to let $\varphi_0 = \pi/2$, Eq. (5) can be rewritten as

$$i_{\mathrm{PD}} \propto 2J_0J_1 \sin\left(2\alpha + \frac{1}{2}D_\omega\omega_{\mathrm{m}}^2\right)\cos[\omega_{\mathrm{m}}(t-\tau_0)]. \quad (6)$$

As can be seen from Eq. (6), the obtained current is proportional to a coefficient $\eta = \sin(2\alpha + 1/2D_\omega{\omega_m}^2)$, so the power varies periodically as the square of the angular frequency ω_m. To construct a low-loss link at a desired frequency, we should let $|\eta|$ equal one, i.e.,

$$2\alpha + \frac{1}{2}D_\omega\omega_{\mathrm{m}}^2 = (2k+1)\frac{\pi}{2}, \qquad k = 0, \pm1, \pm2\cdots. \quad (7)$$

For a given APL, the center frequency ω_m of the analog signal and the length of the link is known. Equation (7) can be easily satisfied if the polarization state of the optical signal introduced to the modulator is carefully adjusted by a PC placed before the PolM. When Eq. (7) is satisfied, the peak of the frequency response of the APL can be shifted to ω_m and the power fading around this frequency can be reduced.

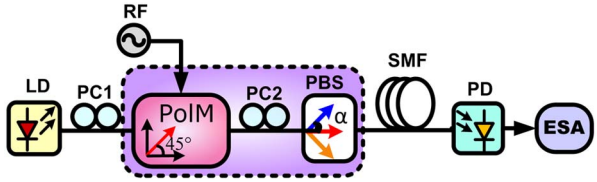

Fig. 2. (Color online) Experiment setup of the polarization-modulated APL. LD, laser diode; PC, polarization controller; PBS, polarization beam splitter; SMF, single-mode fiber; PD, photodetector; ESA, electrical spectrum analyzer.

An experiment is performed based on the setup shown in Fig. 2. Since the integrable modulator has not been fabricated, we implement it by an equivalent setup using separated devices consisting of a PC (PC2), a PolM, and a polarization beam splitter (PBS), which serves as a polarizer. A second PC (PC1) is placed before the PolM to align the polarization direction of the incident light with an angle of 45° to one principal axis of the PolM. In the equivalent modulator, PC2 is adjusted to align the principal axis of the PBS to have an angle of α to one principal axis of the PolM. After transmission over 20 or 40 km SMF, the optical signal is sent to a PD with a responsivity of 0.65 A/W and a 3 dB bandwidth of 40 GHz. The frequency response of the proposed APL is measured by a vector network analyzer, the electrical spectra are observed by an electrical spectrum analyzer (Agilent E4447AU), and the eye diagrams are measured by a sampling oscilloscope (Agilent 86100A).

Figure 3 shows the frequency responses of the polarization-modulated link with 20 or 40 km SMF. As a comparison, the frequency responses of a conventional IM-based link with the same length of SMF are also plotted. For the IM-based link, the ratio between the amplitude modulation and phase modulation is fixed, so signals at certain frequencies (e.g., 14.64 and 33.95 GHz in the 20 km link and 15.36 and 28.09 GHz in the 40 km link) would undergo serious CD-induced power fading. On the contrary, the ratio between the amplitude modulation and phase modulation in the polarization-modulated link can be easily adjusted by the PC to eliminate the power fading at any desired frequency. For instance, we successfully change the frequency responses from the notches in the IM link to peaks in the proposed link, as shown in Fig. 3.

In order to evaluate the transmission performance, a microwave signal with data modulation is distributed in the proposed APL and the IM-based link with 20 km

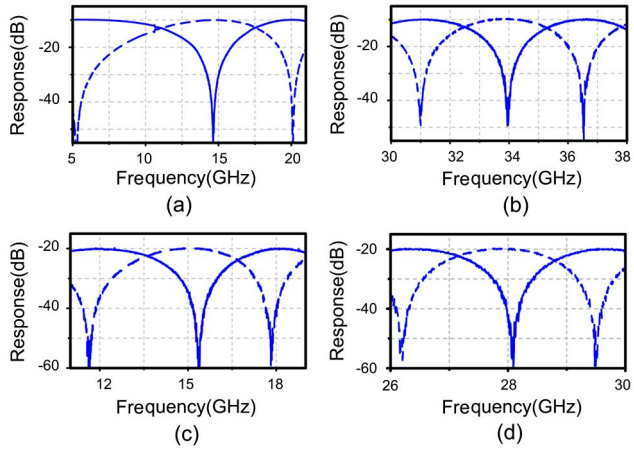

Fig. 3. (Color online) Frequency responses of the conventional IM-based link (solid) and the proposed APL (dashed) after transmission (a) over 20 km SMF around 15 GHz, (b) over 20 km SMF around 34 GHz, (c) over 40 km SMF around 15 GHz, and (d) over 40 km SMF around 28 GHz.

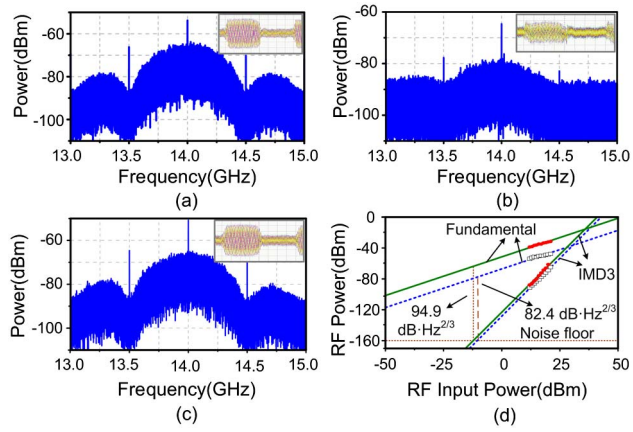

Fig. 4. (Color online) Eye diagrams and electrical spectra of the data-modulated microwave signals transmitted in (a) the conventional IM-based back-to-back link, (b) the conventional IM-based link with 20 km SMF, and (c) the proposed APL with 20 km SMF. (d) Measured fundamental and third-order intermodulation distortion (IMD3) output powers as a function of the input power for the conventional IM-based link with 20 km SMF (dotted line) and the proposed APL with 20 km SMF (solid line).

SMF. The microwave signal is generated by mixing a 500 Mb/s pseudorandom bit sequence with a 14 GHz sinusoidal signal at an electrical mixer. Figures 4(a)–4(c) show the eye diagrams and the electrical spectra of the signals in the two 20 km links. The electrical spectrum is significantly attenuated for the IM-based link. Correspondingly, the eye diagram is distorted, as shown in the inset of Fig. 4(b). For the polarization-modulated link, however, both the eye diagram and the electrical spectrum almost keep the same as the back-to-back case, as shown in Fig. 4(c), indicating that the compensation of the dispersion-induced power fading around 14 GHz greatly improves the transmission performance.

The SFDRs of the IM-based link and the proposed APL with 20 km SMF are also measured. A two-tone signal centered at 14 GHz with a separation of 20 MHz is generated by a vector signal generator (Agilent E8267D) and sent to the PolM via its RF port. As shown in Fig. 4(d), the SFDRs of the two linksare 82.4 and 94.9 dB · $Hz^{2/3}$ when the noise floor is −160 dBm/Hz, indicating that the compensation of the dispersion-induced power fading in the proposed APL increases the SFDR as large as 12.5 dB as compared with the conventional IM-based link.

In conclusion, a novel integrable modulator for APLs with compensation of the dispersion-induced power fading was proposed and demonstrated. The power fading at any frequency of interest could be compensated by adjusting a PC placed before the modulator, which significantly improves the performance of the APLs. The proposed APL may find applications in radar systems, wireless communications, and phased array antennas.

This Letter was supported in part by the National Basic Research Program of China (973 Program) under grant 2012CB315705; the National Natural Science Foundation of China under grants 61107063, 61090392, and 60877043; the National "863" Project under grant 2011AA010305; the Program for New Century Excellent Talents in University (NCET); and the Ph.D. Programs Foundation of the Ministry of Education of China under grant 20113218120018.

References

1. V. J. Urick, F. Bucholtz, J. D. McKinney, P. S. Devgan, A. L. Campillo, J. L. Dexter, and K. J. Williams, J. Lightwave Technol. **29**, 1182 (2011).
2. J. Park, W. V. Sorin, and K. Y. Lau, Electron. Lett. **33**, 512 (1997).
3. J. Li, T. G. Ning, L. Pei, C. H. Qi, X. D. Hu, and Q. Zhou, IEEE Photon. Technol. Lett. **22**, 516 (2010).
4. S. R. Blais and J. P. Yao, IEEE Photon. Technol. Lett. **18**, 2230 (2006).
5. G. H. Smith, D. Novak, and Z. Ahmed, IEEE Trans. Microwave Theory Tech. **45**, 1410 (1997).
6. C. Lim, A. Nirmalathas, K. L. Lee, D. Novak, and R. Waterhouse, J. Lightwave Technol. **25**, 1602 (2007).
7. B. Hraimel, X. P. Zhang, Y. Q. Pei, K. Wu, T. J. Liu, T. F. Xu, and Q. H. Nie, J. Lightwave Technol. **29**, 775 (2011).
8. Z. Z. Tang, S. L. Pan, and J. P. Yao, "A high resolution optical vector network analyzer based on a wideband and wavelength-tunable optical single-sideband modulator," Opt. Express, submitted for publication.
9. G. H. Nguyen, J. Poette, and B. Cabon, J. Lightwave Technol. **29**, 1753 (2011).
10. S. Y. Li, X. P. Zheng, H. Y. Zhang, and B. K. Zhou, Opt. Lett. **36**, 546 (2011).
11. S. L. Pan and J. P. Yao, IEEE Photon. Technol. Lett. **21**, 929 (2009).
12. B. M. Haas and T. E. Murphy, IEEE Photon. Technol. Lett. **19**, 729 (2007).
13. J. P. Yao, F. Zeng, and Q. Wang, J. Lightwave Technol. **25**, 3219 (2007).